DR MARINA MONTRESOR (Orcid ID : 0000-0002-2475-1787)

Article type : Regular Manuscript

Virus-induced spore formation as a defense mechanism in marine diatoms

Angela Pelusi[1], Pasquale De Luca[2], Francesco Manfellotto[1], Kimberlee Thamatrakoln[3*], Kay D. Bidle[3*], Marina Montresor[1*]

[1] Department of Integrative Marine Ecology, Stazione Zoologica Anton Dohrn, Villa Comunale, 80121 Naples, Italy

[2] Research Infrastructures for Marine Biological Resources, Stazione Zoologica Anton Dohrn, Villa Comunale, 80121 Naples, Italy

[3] Department of Marine and Coastal Sciences, Rutgers University, 08901 New Brunswick, New Jersey, USA

*Marina Montresor, orcid.org/0000-0002-2475-1787, e-mail: marina.montresor@szn.it Tel: x39 081 5833259

*Kimberlee Thamatrakoln, orcid.org/0000-0002-8029-5026, e-mail: thamat@marine.rutgers.edu Tel: x1 (848) 932-3464

*Kay D. Bidle, orcid.org/0000-0003-4170-412X, e-mail: bidle@marine.rutgers.edu Tel: x1 (848) 932-3467

Received: 23 July 2020
Accepted: 9 September 2020

Angela Pelusi, orcid.org/0000-0001-9038-0606
Pasquale De Luca: orcid.org/0000-0003-4289-6784
Francesco Manfellotto: orcid.org/0000-0001-9032-3783

Summary

- Algal viruses are important contributors to carbon cycling by recycling nutrients and organic material through host lysis. Although viral infection has been described as a primary mechanism of phytoplankton mortality, little is known about host defense responses.
- We show that viral infection of the bloom-forming, planktonic diatom *Chaetoceros socialis* induces the mass formation of resting spores, a heavily silicified life cycle stage associated with carbon export due to rapid sinking.
- Although viral RNA was detected within spores, mature virions were not observed. 'Infected' spores were capable of germinating, but did not propagate or transmit infectious viruses.
- These results demonstrate that diatom spore formation is an effective defense strategy against viral-mediated mortality. They provide a possible mechanistic link between viral infection, bloom termination, and mass carbon export events and highlight an unappreciated role of viruses in regulating diatom life cycle transitions and ecological success.

Keywords

Chaetoceros socialis, diatoms, life cycle, single-stranded RNA virus, resting spores

Introduction

Many unicellular eukaryotes are characterized by heteromorphic life histories that include different morphological and physiological stages. Examples include organisms that have a haplo-diplobiontic life cycle (von Dassow *et al.*, 2009), can form multi-cellular colonies or chains (Peperzak & Gäbler-Schwarz, 2012), or have the capability to form quiescent or dormant stages such as resting cysts, spores, or akinetes (Ellegaard & Ribeiro, 2018). Heteromorphic life cycles can increase the range of conditions in which a species can survive or act as a defense strategy against predators and/or pathogens (Pančić & Kiørboe, 2018).

Resting stages are present in the life cycles of species that are widely distributed over the broad phylogenetic diversity of microalgae. Their distinctive features include the inability to reproduce (undergo binary fission), and a series of morphological and physiological traits, such as thick cell walls, high concentration of lipids and carbohydrates, and low metabolic activity, all of which allow for dormancy or quiescence for extended periods of time (Ellegaard & Ribeiro, 2018). The formation of resting stages has been linked to the onset of adverse environmental conditions, such as lack of nutrients, changes in temperature or day length (Kuwata *et al.*, 1993; Kremp *et al.*, 2009), or food limitation for heterotrophic and mixotrophic species (Tillmann & Hoppenrath, 2013). In diatoms, resting spores play an important role in community structure and population dynamics, acting as 'seed banks' and allowing species to subsist under sub-optimal conditions until more favourable environments return. The physiological transition to spores has also been implicated in mass export events following diatom blooms due to their heavily silicified, thick frustules that facilitate rapid sinking (Salter *et al.*, 2012; Rynearson *et al.*, 2013; Rembauville *et al.*, 2016).

There are limited studies on the role of biotic interactions as triggers for resting stage formation. Infection of the dinoflagellate *Scrippsiella trochoidea* by the parasite *Amoebophrya* accelerated the formation of resting cysts that were resistant to further parasitic attacks (Chambouvet *et al.*, 2011). Similarly, exposure of *Alexandrium ostenfeldii* to water-borne chemical cues produced by the parasitic flagellate *Parvilucifera infectans* induced the formation of temporary cysts (Toth *et al.*, 2004). Infection by viruses as a trigger for resting spore formation has not been extensively explored, in part because viruses have historically been considered to mediate the recycling of

particulate organic matter through lysis of their host – a process referred to as the "viral shunt" (Wilhelm & Suttle, 1999). However, recent findings suggest viruses may also act as "shuttles" of carbon to depth by altering host physiology, enhancing the production of polysaccharidic, transparent exopolymer particles (TEP) (Nissimov *et al.*, 2018) or proteinaceous coomassie staining particles (CSPs) (Yamada *et al.*, 2018), which serve to facilitate the aggregation of ballasted phytoplankton (Laber *et al.*, 2018). Given the aforementioned link between spores and export flux, a possible role of viral infection in spore formation could represent an unappreciated mechanism facilitating carbon flux out of the surface ocean.

Here, we investigated and quantified the dynamics of spore formation during viral infection of the marine planktonic diatom *Chaetoceros socialis* (Tomaru *et al.*, 2009) using two host strains isolated from geographically distinct regions (Italy and Japan). We show that infection induces the transformation of vegetative cells into resting spores and that spores dramatically minimize the propagation of infectious viruses upon germination. Our results suggest that spore formation is a defense strategy against stressful biotic interactions with impacts for viral-mediated carbon export and the ecological persistence of diatom populations in the face of pervasive viral pressure.

Materials and Methods

Maintenance of *Chaetoceros socialis* hosts and virus

Two strains of *Chaetoceros socialis* Lauder were used in this study. *C. socialis* strain APC12 was isolated in 2015 from a single short chain of cells that had germinated during incubations of surface sediments collected in the Gulf of Naples (Mediterranean Sea, Italy). The strain is preserved as dormant spores (Pelusi *et al.*, 2019) and freshly established cultures were used for all experiments. Strain L-4 (identified as *C. socialis* f. *radians*) was isolated in 2005 from Hiroshima Bay, Japan and kindly provided by Dr. Yuji Tomaru (National Research Institute of Fisheries and Environment of Inland Sea, Fisheries Research Agency). The D1-D3 region of the nuclear encoded large subunit ribosomal DNA of the two strains was sequenced as described in (Gaonkar *et al.*, 2017) (L-4 GenBank accession number: MT919894; APC12 GenBank accession number: MK765996). The two sequences have been added to the alignment in (Gaonkar *et al.*, 2017) and a maximum likelihood

phylogenetic tree was constructed. Cultures were maintained in f/2 medium (Guillard, 1975), prepared with artificial seawater (Sigma-Aldrich St. Louis, USA) containing a modified N:P molar ratios of ~20 and a slightly higher silicate concentration (580 µM NO_3, 29 µM PO_4, 360 µM SiO_4), at 18 °C on a 12 h:12 h, light : dark photoperiod at 80 µmol photons m^{-2} s^{-1}. The virus used in this study was CsfrRNAV01, a single-stranded RNA virus recently reclassified into the genus *Bacillarnavirus* (Vlok *et al.*, 2019) and documented to specifically infect strain L-4 (Tomaru *et al.*, 2009). Virus lysates were generated by infecting cultures of strain L-4 until host lysis, then removing cellular debris by filtration using a 0.22 µm pore-size polycarbonate filter (Millex-GV Millipore, Merck). The resulting virus lysate had $1.70 \cdot 10^6$ viral gene copies ml^{-1}, as assessed with qRT-PCR and was stored at -80 °C until use.

Experimental set-up

All experiments were carried out in triplicate at 18°C, 180 µmol photons m^{-2} sec^{-1}, and on a 12 h :12 h, light : dark photoperiod. Cultures were grown to early exponential phase (~ $6 \cdot 10^4$ cells ml^{-1}), infected with the viral lysate (100:1 v:v) and monitored daily for cell concentration and chlorophyll fluorescence. Uninfected cultures were maintained as controls. The concentration of both vegetative cells and spores was measured on fixed (1.6% final concentration of a neutral formaldehyde solution) subsamples of each replicate, using a Sedgewick-Rafter chamber and a Zeiss Axiophot microscope (ZEISS, Oberkochen, Germany) at 400x magnification. Chlorophyll fluorescence (relative fluorescence units; RFUs) was measured at the same time of the day using a Turner Designs fluorometer (model 10-005R, Turner Designs, INC. Sunnyvale, CA, USA).

Nitrogen starvation, a known abiotic factor that induces spore formation (Pelusi *et al.*, 2019), was used as control to test spore formation dynamics. Exponentially growing cultures were inoculated in triplicate flasks at an initial cell concentration of 3,000 cells·ml^{-1} in f/2 culture medium with low nitrogen content (23 µM nitrate). Cell and spore abundance was monitored for 5 days.

For germination experiments, cleaned spores (see 'Isolating and cleaning spores') were re-suspended in f/2 medium in triplicate glass tubes and placed in the dark for one week. They were moved to the light under standard experimental conditions and monitored for growth by chlorophyll fluorescence.

Isolating and cleaning spores

Cultures with microscopically-verified spores were sonicated 3x on ice for 1 min with a Branson 250 sonicator (100 W) to break up vegetative cells into smaller pieces and then filtered onto 1.2 μm pore-size polycarbonate filters (RAWP04700 Millipore). Filters were washed three times with 50 mL of sterile ASW to remove any free viruses and cell debris. Samples were collected before and after washing and assayed via the most probable number (MPN) assay to determine the number of infectious viruses. A subsample was also collected to measure the concentration of clean spores.

Quantifying virus abundance

Virus abundance was assessed using MPN to measure the number infectious viruses (i.e., the number of viruses capable of infecting a new host) and quantitative real time polymerase chain reaction (qRT-PCR) to measure the number of viral gene copies. For MPN, individual wells in a 96-well plate were filled with 240 μl of strain APC12 or L-4 at cell concentrations of ~$3 \cdot 10^5$ cells·ml^{-1} using a Freedom EVO (Tecan, Männedorf, Switzerland) platform. A total of ten, 10-fold serial dilutions were prepared from the viral lysate and 10 μl of each dilution was transferred into 8 wells containing the host culture. Inoculation with only growth medium served as a negative control; undiluted virus lysate served as a positive control. Microtiter plates were incubated at standard experimental conditions and checked daily with an Infinite M1000 Pro microplate reader (Tecan, Männedorf, Switzerland) until cultures infected with undiluted virus lysate became clear (no more than 15 days). Scores were defined positive when samples were cleared; the infectious viral units·mL^{-1} was calculated using the EPA-MPN Calculator 2.0 (Klee, 1993).

For qRT-PCR measurements of total extracellular virus concentration, 1.5 ml of cultures were filtered through a 0.22 Sterivex GV filter unit (Millipore) and filtrates were stored at -80 °C until nucleic acid extraction. For determination of intracellular viruses, cells or spores (~$5.8 \cdot 10^6$ total cells/spores) were collected onto 1.2 μm pore-size polycarbonate filters (RAWP04700 Millipore) and then immediately submerged into 1 ml of TRIzol® Reagent (Invitrogen, Carlsbad, California) and stored at -80 °C until nucleic acid extraction.

Extraction of viral nucleic acids

For extracellular viral nucleic acid extraction, chloroform (1:50 v:v) was added to thawed lysates and mixed on a shaker for 10 min at room temperature (RT). The samples were centrifuged at 11,900 rcf for 20 min at RT and the supernatant containing the viral particles was transferred into new microfuge tubes and treated with both RNase and DNase (1 $\mu g \cdot mL^{-1}$ final concentration) for 30 min at 37 °C to avoid contamination of nucleic acids from host cells. Viral particles were precipitated overnight at 4 °C in an equal volume of 20% (w:v) polyethylene glycol (PEG) 8000 in 2.5 M NaCl. Samples were then centrifuged (11,900 rcf; 30 min; 4 °C) and the pellets were re-suspended in 0.5 ml of TRIzol® Reagent (Invitrogen, Carlsbad, California) for RNA extraction, following manufacturer's instructions. The resulting RNA pellet was dried, resuspended in RNase free water, treated with RNase-free DNase I (Roche) and further purified on Qiagen columns (74104, RNeasy Mini Kit) following the manufacturers' protocol. RNA was quantified with a NanoDrop ND-1000 Spectrophotometer (Nanodrop Tecnologies Inc., Wilmington, USA). A volume of 12 µl for each sample was used to synthesize cDNA trough qScript™ XLT cDNA SuperMix (Quanta BioScience, Inc) following the manufacturers' protocol. Primer sequences specific for the gene encoding non-structural polyprotein CSfrRV_gp1 were designed using available sequence information at NCBI (https://www.ncbi.nlm.nih.gov/gene/7559143) and the Primer3Plus version 2.4.2 (Untergasser *et al.*, 2012). The sequences for the forward and reverse primers are 5'-TCGACAAGAACCAAGCACAG-3' and 5'-GTCCCCAAAGTGGTTGAGAA-3', respectively, yielding a 192 bp PCR product. The procedure for extracting intracellular viral nucleic acids from host cells collected onto filters was the same as above, with the only differences being the amount of total RNA used for reverse transcription that was 150 ng and the fact that samples were not pre-treated with RNase or DNase. To test if the viral genome was inserted into the host genome as a stable DNA sequence (via lysogeny), we collected a subsample of viral-induced spores, extracted DNA following (Gaonkar *et al.*, 2017) and amplified it as described below.

PCR and quantitative reverse-transcription PCR (qRT-PCR)

PCR reactions for he non-structural polyprotein (CSfrRV_gp1) contained the following reagents: 0.4 µM of forward and reverse primers, 2 µl of template, 5x XtraWhite buffer solution (GeneSpin,

Milano, Italy), 0.2 mM of dNTPs, 1.12 U of XtraTaq Pol (GeneSpin, Milano, Italy) and water to a final volume of 20 µl. Thermal cycling conditions were as follows: 2 min at 95 °C followed by 35 cycles of 15 sec at 95 °C and 30 sec at 58 °C, 30 sec at 72 °C and 7 min at 72 °C. The PCR products were then run on an agarose gel (1.2%) and the resulting amplicons were purified by GenElute gel extraction kit (Sigma Chemical, St. Louis, MO) following manufacturer's protocol. One amplicon fragment from both RNA and DNA source material was sequenced using an Ion Proton sequencer (Life Technologies, Carlsbad, USA) with an Ion P1 sequencing kit v2 and searched against the GeneBank database.

The qRT-PCR reactions contained the following: 5 µl of 2× Power SYBR Green Master Mix (containing buffer, dNTPs, SYBR Green I, AmpliTaq Gold DNA Polymerase LD and Passive Reference; Thermo Fisher Scientific), 0.7 µM of forward and reverse primers, 1 µl of template cDNA, and RNAse-free water to a final volume of 10 µl. Reactions were performed on a ViiA™ 7 Real-Time PCR System with 384-Well Block using the following thermal cycling conditions: 10 min at 95 °C, followed by 40 cycles of 15 s at 95 °C and 1 min at 60 °C, with the addition of a melting curve to assess the potential amplification of non-specific products. Fluorescence was detected at the end of each cycle with the automatic determination of the threshold cycle (C_t). A serial dilution of a viral reverse transcript sample was employed to construct a standard curve to quantify products. The viral copy number was calculated with empirical formulas previously described (Tomaru & Kimura, 2016). Virus burst size was calculated by dividing the total number of viruses produced by the number of host vegetative cells lost (i.e., maximum host abundance minus final host abundance) as follows: (final virus concentration (T_f) – initial virus concentration (T_0))/(maximum concentration of vegetative cells in exponential phase prior to lysis – final concentration of vegetative cells after lysis phase).

Transmission Electron Microscopy

Infected APC12 cells were collected for transmission electron microscopy (TEM) analysis using a previously described protocol (Zingone *et al.*, 2006), with the exception that sections were stained with UAR-EMS Uranyl Acetate Replacement Stain diluted 1:4 (v:v). Thin sections were examined with a Zeiss Leo 912 AB transmission electron microscope (Karl Zeiss, Oberkochen, Germany). TEM

preparations of extracellular virus-like particles were made by adding chloroform (1:50 v:v) to lysates and incubating for 10 min at 37 °C shaking at 600 rpm. The sample was then centrifuged (17,900 rcf; 20 min; RT) to eliminate cellular debris. The resulting supernatant was mixed with an equal volume of 20% (w:v) polyethylene glycol (PEG) 8000 in 2.5 M NaCl and incubated overnight at 4°C. This sample was centrifuged (17,900 rcf; 30 min; 4°C) and the pellet resuspended in 10 µL of SM buffer (NaCl 100 mM; $MgSO_4 \cdot 7H_2O$ 8 mM; Tris-Cl (1 M, pH 7.5) 50 mM, H_2O). The virus suspension was mounted on a Formvar-Carbon coated grid for 30 s and excess solution was removed with blotting paper. The sample was stained for 10 s with 10 µl of 2% phosphotungstic acid. After the removal of excess dye, the grid was dried in a chemical hood for 2 days and examined on a Zeiss LEO 912 AB (Zeiss, Oberkochen, Germany) microscope.

Statistical analysis

A two–tailed Mann-Whitney U test was used to evaluate i) the difference in concentration of viral particles and infectious units at the end of experiments and ii) the differences between the percentage of spores in infected and uninfected cultures of the two strains. Values were defined significantly different when $p<0.05$. Statistical tests were performed with GraphPad Prism 6.

Results

Host susceptibility to viral infection

We tested the infection dynamics of two geographically distinct strains of *Chaetoceros socialis,* one isolated from surface sediments in the Gulf of Naples, Mediterranean Sea, Italy (strain APC12) and the other from Hiroshima Bay, Japan (strain L-4; Fig. 1a-c). Given the cryptic diversity reported for *C. socialis* species complex (Chamnansinp *et al.*, 2013; Gaonkar *et al.*, 2017), we tested the genetic relatedness of these strains by sequencing the D1-D3 region of the nuclear encoded large subunit ribosomal DNA. The two sequences were 99% identical to the type sequence of *C. socialis* [strain YL1 in (Chamnansinp *et al.*, 2013)] and were firmly placed within this species clade (Fig. 1d).

The single-stranded RNA virus, CsfrRNAV, was originally isolated with *C. socialis* strain L-4 (Tomaru *et al.*, 2009). Given the high species and, in some cases, strain specificity observed in other

diatom host-virus systems (Kimura & Tomaru, 2015), we tested whether CsfrRNAV could infect APC12 cells, with L-4 serving as positive control (Fig. 2a). Infection of L-4 caused host demise 3 days post-infection (dpi) (Fig. 2a), consistent with previous observations (Tomaru *et al.*, 2009). CsfrRNAV also successfully infected APC12 with similar dynamics to L-4, causing a decline in host abundance 3 dpi. Both host strains produced a similar number of viruses, measured by either qRT-PCR ($p=0.700$) of the CSfrRV-derived non-structural polyprotein (CSfrRV_gp1) gene or most probable number (MPN) assay ($p=0.700$), which respectively represent the total and infectious virus abundance (Fig. 2b, c). Upon host lysis, extracellular virus abundance increased four orders of magnitude for L-4 and six for APC12, with an average of $1.98 \cdot 10^{10} \pm 1.05 \cdot 10^{9}$ and $6.57 \cdot 10^{11} \pm 5.46 \cdot 10^{11}$ viral gene copies$\cdot$ml^{-1}, respectively (Fig. 2b). Infectious units for both strains were considerably lower (Fig. 2c), with average values of $3.05 \cdot 10^{6} \pm 1.40 \cdot 10^{6}$ infectious units$\cdot$ml^{-1} in L-4 (< 0.02% of the total viral abundance) and $5.34 \cdot 10^{6} \pm 1.92 \cdot 10^{6}$ infectious units$\cdot$ml^{-1} in APC12 (<0.03% of the total viral abundance). Burst size for strain L-4 was $6.12 \cdot 10^{4}$ and for APC12 was $1.18 \cdot 10^{6}$. Transmission electron microscopy of ultra-thin sections of infected strain APC12 confirmed the presence of virus-like particles within vegetative cells (Fig. 2 d, e), along with extracellular viruses, polyhedral in shape, with a diameter ranging between 20-22 nm (Fig. 2f). Collectively, these findings demonstrate that CsfrRNAV could successfully infect, replicate, and produce viral progeny in a geographically distinct strains of *C. socialis*.

Virus-induced spore formation

The drop in cell abundance during virus infection of APC12 was concurrent with a notable increase in spore formation compared to the uninfected control ($p=0.006$), with an average of $48.1 \pm 6.38\%$ of cells transitioning to spores 4 dpi (Fig. 3a, b). Induction of spores was much lower in infected L-4 cultures, with only ~5% of cells becoming spores 4 dpi (Fig. 3c, d). To contextualize these findings, we tested the ability of both APC12 and L-4 to form spores under nitrogen (N) limitation, a treatment known to induce a shift from vegetative cells to resting stages in most diatoms, including *C. socialis* (Pelusi *et al.*, 2019). Less than 1% of the cells of strain L-4 formed spores after five days in N-limited medium, compared to $99\% \pm 0.69$ in strain APC12 (Supporting Information Fig. S1), indicating that L-4 has markedly lower ability to form resting stages than APC12. Given APC12 represented a

susceptible host strain capable of forming prominent spores, we further characterized the relationship between viral infection and spore formation in this strain.

We characterized the temporal dynamics of spore formation and host/viral abundance during infection (Supporting Information Fig. S2). Intracellular virus abundance increased 2 dpi and reached a maximum of $1.22 \cdot 10^4 \pm 9.08 \cdot 10^3$ viral gene copies$\cdot$cell^{-1} on day 4. The initial increase in intracellular virus abundance coincided with a detectable increase in extracellular virus abundance, with the latter increasing to $1.10 \cdot 10^8 \pm 4.02 \cdot 10^7$ 4 dpi (Supporting Information Fig. S2b). Spores were detected 2 dpi, reaching nearly 80% of the culture by day 4. To determine whether viruses were associated with spores, we isolated cleaned spores on day 7 (see the Materials and Methods section) and performed qRT-PCR. Amplification of CSfrRV_gp1 was detected in infection-induced spores (Fig. 3e-f) with an average viral copy number of $9.17 \cdot 10^4 \pm 2.27 \cdot 10^4 \cdot$spore^{-1}. No amplification was observed in uninfected vegetative cells (Fig. 3f) or in spores generated by N-limitation (Fig. 4a). We also assessed whether the ssRNA virus genome was integrated into the host genome, as has been observed for some RNA viruses (Ciuffi, 2016). We found no evidence of CsfrRV_gp1 amplification from host genomic DNA extracted from virus-induced spores. Despite the high viral gene copies associated with spores, no mature virus-like particles were observed via TEM (Fig. 3g).

The high intracellular viral abundance in both vegetative cells and spores led us to posit that infected spores may propagate viruses upon germination. A subsample of spores, which were confirmed to contain viral RNA (Fig. 4a), were collected and washed thoroughly to remove free, extracellular viruses prior to inoculating into fresh medium at a concentration of $1.1 \cdot 10^4$ spores ml^{-1}. MPN assays confirmed a 99.7% drop in extracellular viral abundance after washing (Fig. 4b) providing confidence that there was minimal carry-over of free viruses. Spores germinated after 5 days, as indicated by an increase in chlorophyll fluorescence, and grew until a peak abundance on day 10, after which chlorophyll fluorescence decreased (Fig. 4c). Extracellular virus abundance measured on day 14 was barely detectable at only 0.16 ± 0.04 infectious units ml^{-1} (Fig. 4b), arguing that the decrease in host abundance was not due to viral-mediated mortality. Intriguingly, the dynamics of spore germination and growth was noticeably different than that for spores induced by N-limitation, which germinated much faster, within one day, and peaked by day 3 (Fig. 4c). Taken together, these data suggest that virus-induced spores are capable of germinating, albeit at a slower rate, but that they

are not capable of transmitting infective viruses upon germination and likely harbour immature viruses that are incapable of replication and assembly.

Discussion

We found that two geographically distant, but genetically identical, strains of *C. socialis,* APC12 (Mediterranean) and L-4 (Hiroshima Bay, Japan), were both successfully infected by the ssRNA virus CsfrRNAV, originally isolated from strain L-4. Infection dynamics were similar between the two strains, with host lysis observed 3 dpi, and similar numbers of total (10^{10}-10^{11} viruses·ml^{-1}, quantified by qRT-PCR) and infectious (~10^{6} viruses·ml^{-1}, quantified by MPN) viruses produced. The much lower number of infectious viruses compared to the total (0.01-0.001%) was noteworthy and similar to observations in other unicellular hosts (Van Etten *et al.*, 1983; Cottrell & Suttle, 1995; Bratbak *et al.*, 1998). This discrepancy remains an important consideration when contextualizing the potential ecological impact of total virus abundances in different systems. Despite similar viral production between the two host strains, the respective burst sizes (the number of total viruses produced per host cell) were markedly different; the burst size of APC12 was >15-fold higher than L-4, suggesting viral replication was more productive in APC12. The mechanism behind enhanced intracellular replication in APC12 is unknown, but it resembles facilitated replication in plants and animals in which naïve hosts with no known previous exposure to a particular virus exhibit enhanced viral production upon infection (Jones, 2009).

Given that the majority of isolated diatom viruses have high species, and in many cases, strain-specificity (Nagasaki *et al.*, 2004; Tomaru *et al.*, 2009; Arsenieff *et al.*, 2019), these findings highlight that host-virus specificity is not regionally limited. Only one virus to date, CtenRNAV type-II, has been shown to infect different *Chaetoceros* species (Kimura & Tomaru, 2015). However, strain specificity within a population is more commonly reported, as is the case with viruses that infect *C. debilis* (Tomaru *et al.*, 2008) or *Guinardia delicatula* (Arsenieff *et al.*, 2019). Infection of hosts isolated from different geographic areas has been observed in other microalgal species, such as the prasinophycean *Micromonas pusilla* (Zingone *et al.*, 2006), the prymnesiophycean *Phaeocystis globose* (Baudoux & Brussaard, 2005), and the dinoflagellate *Heterosigma akashiwo* (Tai *et al.*,

2003), but to our knowledge, this is the first report of a diatom virus capable of infecting con-specific strains from distant locations. Taken together, these findings highlight variable intra-species specificity of algal viruses and illustrates the need for better understanding the mechanisms regulating host susceptibility and resistance (Short, 2012).

Abiotic environmental factors, such as light, temperature, and nutrient regime, are well-known drivers of resting stage formation in unicellular eukaryotes (McQuoid & Hobson, 1996; Figueroa *et al.*, 2018). Little is known about biotic interactions that trigger spore formation, in particular viruses, which are widespread and persistent biological stressors. Here, we observed that infection of the Mediterranean strain of *C socialis* (APC12) induced up to ~80% of the culture to form spores demonstrating that viral infection can trigger spore formation in diatoms. The lack of appreciable spore formation in the Japanese strain (L-4) in response to infection or N-limitation suggests that either this strain has an intrinsically lower ability to form spores as compared to APC12 or that its ability has been reduced by prolonged time in culture. The impact of long-term culturing on various life history traits has been widely observed across taxonomic groups including dinoflagellates that have lost the ability to form resting cysts, diatoms that display reduced sexuality, and prymnesiophytes that have lost the ability to form a calcified diploid stage (Lakeman *et al.*, 2009). Although a previous study qualitatively reported viral-induced spore formation in L-4, we note that spores were only observed 23 dpi, well into nutrient limiting conditions and far outside of the time frame of lytic infection (Tomaru *et al.*, 2009).

Regardless, our findings in APC12 demonstrate viral infection can induce significant spore formation within days of infection, providing evidence for an unappreciated biotic trigger of resting stage formation in diatoms. Although spores were associated with >9 fold higher intracellular viral gene copies than vegetative cells, the lack of visual evidence of mature virions within the cytoplasm suggests that upon infection, a significant pool of viruses started to replicate, but were unable to mature into viable virions upon transition of the host into spores. We posit that in the environment, heavily silicified spores induced by viral infection would rapidly sink out of the surface ocean, effectively removing a subpopulation from the water column and protecting it within sediments. 'Infected' spores could subsequently germinate under nutrient replete conditions providing a seed population for future blooms.

The inability of spores to produce infectious viruses suggests the life cycle shift represents an effective defense strategy, allowing a large fraction of the population to avoid viral-induced mortality. A viral-induced life cycle transition has also been observed in the coccolithophore, *Emiliania huxleyi*, where the presence of large dsDNA *Coccolithoviruses* causes the host to shift from a susceptible, diploid, coccolith-bearing phase to a resistant, haploid, non-calcified, motile phase (Frada *et al.*, 2008; Frada *et al.*, 2012). Virus infection also triggers the appearance of resistant, diploid or aneuploid morphotypes of *E. huxleyi* with lower growth rates than uninfected controls (Frada *et al.*, 2017), an observation that is consistent with our findings of lower growth rates for *C. socialis* cells germinated from infected spores (Fig. 4c). The physiological mechanism(s) driving this indirect negative impact of viral infection on the growth and fitness of future diatom generations remains to be evaluated.

Abundant, widespread signatures of ssRNA viruses have been found throughout the world ocean (Miranda *et al.*, 2016) and diatom viruses have been shown to actively infect natural diatom populations across different nutrient regimes (Moniruzzaman *et al.*, 2017; Kranzler *et al.*, 2019). The induction of spore formation by viral infection provides a novel mechanistic link between diatom bloom termination and mass export events attributed to heavily silicified spores with high sinking rates and aggregation (Rynearson *et al.*, 2013), accompanying recent findings that virus infection may be a dominant driver of carbon export in the ocean (Laber *et al.*, 2018; Kranzler *et al.*, 2019). Although the subcellular mechanisms that regulate the induction of resting spores by viral attack remain to be clarified, our findings add to the ecophysiological and evolutionary arms race that governs host-virus interactions in the oceans (Frada *et al.*, 2008; Bidle & Vardi, 2011; Frada *et al.*, 2012; Bidle, 2015) with spore formation serving to preserve and propagate populations of hosts, while, at the same time, short-circuiting the transmission of viruses to subsequent diatom generations.

Acknowledgments

AP has been supported by a PhD fellowship from Stazione Zoologica Anton Dohrn (SZN) and by a fellowship of the project ABBaCo (Restauro Ambientale e Balneabilità del SIN Bagnoli-Coroglio), funded by the Italian Ministry for Education, University and Research [grant no. C62F16000170001]. This work was partly supported by awards from the Gordon and Betty Moore Foundation

(Investigator Award #3789) and US National Science Foundation (OCE-1537951) to KDB. The authors thank Dr. Yuji Tomaru (National Research Institute of Fisheries and Environment of Inland Sea, Fisheries Research Agency) for providing the *C. socialis* L-4 host and CsfrRNAV, the Electron Microscopy Unit (SZN) for assistance in TEM preparations, the Molecular Biology and Sequencing Unit (SZN) for sequencing, and Carmen Minucci for technical support.

Author Contributions

A.P., K.D.B., K.T. and M.M. designed the study, A.P., P. DL. and F.M. carried out the experiments, A.P., K.D.B., K.T. and M.M. wrote the paper that was discussed with all the authors

References

Alldredge AL, Gotschalk C, Passow U, Riebesell U. 1995. Mass aggregation of diatom blooms: Insights from a mesocosm study. *Deep Sea Research Part II: Topical Studies in Oceanography* **42**(1): 9-27.

Arsenieff L, Simon N, Rigaut-Jalabert F, Le Gall F, Chaffron S, Corre E, Com E, Bigeard E, Baudoux AC. 2019. First viruses infecting the marine diatom *Guinardia delicatula*. *Frontiers in Microbiology* **9**: 3235

Baudoux A-C, Brussaard CP. 2005. Characterization of different viruses infecting the marine harmful algal bloom species *Phaeocystis globosa*. *Virology* **341**(1): 80-90.

Bidle KD. 2015. The molecular ecophysiology of programmed cell death in marine phytoplankton. *Annual Review of Marine Science* **7**(1): 341-375.

Bidle KD, Vardi A. 2011. A chemical arms race at sea mediates algal host-virus interactions. *Current Opinion in Microbiology* **14**(4): 449-457.

Bratbak G, Jacobsen A, Heldal M, Nagasaki K, Thingstad F. 1998. Virus production in *Phaeocystis pouchetii* and its relation to host cell growth and nutrition. *Aquatic Microbial Ecology* **16**: 1-9.

Chambouvet Al, Alves-de-Souza C, Cueff Vr, Marie D, Karpov S, Guillou L. 2011. Interplay between the parasite *Amoebophrya* sp. (Alveolata) and the cyst formation of the red tide dinoflagellate *Scrippsiella trochoidea*. *Protist* **162**(4): 637-649.

Chamnansinp A, Li Y, Lundholm N, Moestrup Ø. 2013. Global diversity of two widespread, colony-forming diatoms of the marine plankton, *Chaetoceros socialis* (syn. *C. radians*) and *Chaetoceros gelidus* sp. nov. *Journal of Phycology* **49**: 1128–1141.

Ciuffi A. 2016. The benefits of integration. *Clinical Microbiology and Infection* **22**: 324-332.

Cottrell MT, Suttle CA. 1995. Genetic diversity of algal viruses which lyse the photosynthetic picoflagellate *Micromonas pusilla* (Prasinophyceae). *Applied and Environmental Microbiology* **61**: 3088-3091.

Ellegaard M, Ribeiro S. 2018. The long-term persistence of phytoplankton resting stages in aquatic 'seed banks'. *Biological Reviews* **93**(1): 166-183.

Figueroa RI, Estrada M, Garcés E. 2018. Life histories of microalgal species causing harmful blooms: Haploids, diploids and the relevance of benthic stages. *Harmful Algae* **73**: 44-57.

Frada M, Probert I, Allen MJ, Wilson WH, de Vargas C. 2008. The "Cheshire Cat" escape strategy of the coccolithophore *Emiliania huxleyi* in response to viral infection *Proceedings of the National Academy of Sciences USA* **105** 15944-15949.

Frada MJ, Bidle KD, Probert I, de Vargas C. 2012. *In situ* survey of life cycle phases of the coccolithophore *Emiliania huxleyi* (Haptophyta). *Environmental Microbiology* **14**(6): 1558-1569.

Frada MJ, Rosenwasser S, Ben-Dor S, Shemi A, Sabanay H, Vardi A. 2017. Morphological switch to a resistant subpopulation in response to viral infection in the bloom-forming coccolithophore *Emiliania huxleyi*. *PLoS Pathogens* 13(12), e1006775.

Gaonkar CC, Kooistra WHCF, Lange CB, Montresor M, Sarno D. 2017. Two new species in the *Chaetoceros socialis* complex (Bacillariophyta): *C. sporotruncatus* and *C. dichatoensis*, and characterization of its relatives, *C. radicans* and *C. cinctus*. *Journal of Phycology* **53**(4): 889-907.

Guillard RRL 1975. Culture of phytoplankton for feeding marine invertebrates. In: Smith WL, Chanley MH eds. *Culture of Marine Invertebrate Animals*. New York: Plenum Press, 29-60.

Jones RA. 2009. Plant virus emergence and evolution: origins, new encounter scenarios, factors driving emergence, effects of changing world conditions, and prospects for control. *Virus Research* **141**(2): 113-130.

Kimura K, Tomaru Y. 2015. Discovery of two novel viruses expands the diversity of single-stranded DNA and single-stranded RNA viruses infecting a cosmopolitan marine diatom. *Applied and Environmental Microbiology* **81**(3): 1120-1131.

Klee AJ. 1993. A computer program for the determination of most probable number and its confidence limits. *Journal of Microbiological Methods* **18**: 91–98.

Kranzler CF, Krause JW, Brzezinski MA, Edwards BR, Biggs WP, Maniscalco M, McCrow JP, Van Mooy BA, Bidle KD, Allen AE. 2019. Silicon limitation facilitates virus infection and mortality of marine diatoms. *Nature Microbiology* **4**(11): 1790-1797.

Kremp A, Rengefors K, Montresor M. 2009. Species specific encystment patterns in three Baltic cold-water dinoflagellates: the role of multiple cues in resting cyst formation. *Limnology and Oceanography* **54**(4): 1125-1138.

Kuwata A, Hama T, Takahashi M. 1993. Ecophysiological characterization of two life forms, resting spores and resting cells, of a marine planktonic diatom, *Chaetoceros pseudocurvisetus*, formed under nutrient depletion. *Marine Ecology Progress Series* **102**: 245-255.

Laber CP, Hunter JE, Carvalho F, Collins JR, Hunter EJ, Schieler BM, Boss E, More K, Frada M, Thamatrakoln K, et al. 2018. Coccolithovirus facilitation of carbon export in the North Atlantic. *Nature Microbiology* **3**(5): 537-547.

Lakeman MB, von Dassow P, Cattolico RA. 2009. The strain concept in phytoplankton ecology. *Harmful Algae* **8**(5): 746-758.

McQuoid MR, Hobson LA. 1996. Diatom resting stages. *Journal of Phycology* **32**: 889-902.

Miranda JA, Culley AI, Schvarcz CR, Steward GF. 2016. RNA viruses as major contributors to Antarctic virioplankton. *Environmental Microbiology* **18**(11): 3714-3727.

Moniruzzaman M, Wurch LL, Alexander H, Dyhrman ST, Gobler CJ, Wilhelm SW. 2017. Virus-host relationships of marine single-celled eukaryotes resolved from metatranscriptomics. *Nature Communications* **8**(1): 16054.

Nagasaki K, Tomaru Y, Katanozaka N, Shirai Y, Nishida K, Itakura S, Yamaguci M. 2004. Isolation and characterization of a novel single-stranded RNA virus infecting the bloom-forming diatom *Rhizosolenia setigera*. *Applied and Environmental Microbiology* **70**(2): 704-711.

Nissimov JI, Vandzura R, Johns CT, Natale F, Haramaty L, Bidle KD. 2018. Dynamics of transparent exopolymer particle production and aggregation during viral infection of the coccolithophore, *Emiliania huxleyi*. *Environmental Microbiology* **20**(8): 2880-2897.

Pančić M, Kiørboe T. 2018. Phytoplankton defence mechanisms: traits and trade-offs. *Biological Reviews* **93**(2): 1269-1303.

Pelusi A, Santelia ME, Benvenuto G, Godhe A, Montresor M. 2019. The diatom *Chaetoceros socialis*: spore formation and preservation. *European Journal of Phycology* **55**(1): 1-10.

Peperzak L, Gäbler-Schwarz S. 2012. Current knowledge of the life cycles of *Phaeocystis globosa* and *Phaeocystis antarctica* (Prymnesiophyceae). *Journal of Phycology* **48**(3): 514-517.

Rembauville M, Manno C, Tarling GA, Blain S, Salter I. 2016. Strong contribution of diatom resting spores to deep-sea carbon transfer in naturally iron-fertilized waters downstream of South Georgia. *Deep-Sea Research Part I-Oceanographic Research Papers* **115**: 22-35.

Rynearson TA, Richardson K, Lampitt RS, Sieracki ME, Poulton AJ, Lyngsgaard MM, Perry MJ. 2013. Major contribution of diatom resting spores to vertical flux in the sub-polar North Atlantic. *Deep Sea Research Part I: Oceanographic Research Papers* **82**: 60-71.

Salter I, Kemp AES, Moore CM, Lampitt RS, Wolff GA, Holtvoeth J. 2012. Diatom resting spore ecology drives enhanced carbon export from a naturally iron-fertilized bloom in the Southern Ocean. *Global Biogeochemical Cycles* **26**, doi.org/10.1029/2010GB003977.

Short SM. 2012. The ecology of viruses that infect eukaryotic algae. *Environmental Microbiology* **14**(9): 2253-2271.

Tai V, Lawrence JE, Lang AS, Chan AM, Culley AI, Suttle CA. 2003. Characterization of HaRNAV, a single-stranded RNA virus causing lysis of *Heterosigma akashiwo* (Raphidophyceae). *Journal of Phycology* **39**(2): 343-352.

Tillmann U, Hoppenrath M. 2013. Life cycle of the pseudocolonial dinoflagellate *Polykrikos kofoidii* (Gymnodiniales, Dinoflagellata). *Journal of Phycology* **49**(2): 298-317.

Tomaru Y, Kimura K. 2016. Rapid quantification of viable cells of the planktonic diatom *Chaetoceros tenuissimus* and associated RNA viruses in culture. *Plankton and Benthos Research* **11**(1): 9-16.

Tomaru Y, Shirai Y, Suzuki H, Nagumo T, Nagasaki K. 2008. Isolation and characterization of a new single-stranded DNA virus infecting the cosmopolitan marine diatom *Chaetoceros debilis*. *Aquatic Microbial Ecology* **50**(2): 103-112

Tomaru Y, Takao Y, Suzuki H, Nagumo T, Nagasaki K. 2009. Isolation and characterization of a single-stranded RNA virus infecting the bloom-forming diatom *Chaetoceros socialis*. *Applied and Environmental Microbiology* **75**(8): 2375-2381.

Toth GB, Norén N, Selander E, Pavia H. 2004. Marine dinoflagellates show induced life-history shifts to escape parasite infection in response to water-borne signals. *Proceedings of the Royal Society B: Biological Sciences* **271**: 733-738.

Untergasser A, Cutcutache I, Koressaar T, Ye J, Faircloth BC, Remm M, Rozen SG. 2012. Primer3-new capabilities and interfaces. *Nucleic Acids Research* **40**(15): e115.

van Etten JL, Burbank DE, Kuczmarski D, Meints RH. 1983. Virus infection of culturable *Chlorella*-like algae and development of a plaque assay. *Science* **219**(4587): 994-996.

Vlok M, Lang AS, Suttle CA. 2019. Marine RNA virus quasispecies are distributed throughout the oceans. *mSphere* **4**(2): e00157-00119.

von Dassow P, Ogata H, Probert I, Wincker P, Da Silva C, Audic S, Claverie JM, de Vargas C. 2009. Transcriptome analysis of functional differentiation between haploid and diploid cells of *Emiliania huxleyi*, a globally significant photosynthetic calcifying cell. *Genome Biology* **10**: R114.

Wilhelm SW, Suttle CA. 1999. Viruses and nutrient cycles in the sea: viruses play critical roles in the structure and function of aquatic food webs. *BioScience* **49**(10): 781-788.

Yamada Y, Tomaru Y, Fukuda H, Nagata T. 2018. Aggregate formation during the viral lysis of a marine diatom. *Frontiers in Marine Science* **5**.

Zingone A, Natale F, Biffali E, Borra M, Forlani G, Sarno D. 2006. Diversity in morphology, infectivity, molecular characteristics and induced host resistance between two viruses infecting *Micromonas pusilla*. *Aquatic Microbial Ecology* **45**(1): 1-14.

Figure legends

Fig. 1 *Chaetoceros socialis* strains used in this study. (a) Isolation sites of strains of *C. socialis*, APC12 (red) and L-4 (blue). (b) Globular arrangement of chains of vegetative cells of strain APC12; bar, 50 µm. (c) Two chains of vegetative cells of strain L-4; bar, 10 µm. (d) Maximum likelihood tree inferred from partial 28S sequences of *Chaetoceros* species (Gaonkar *et al.*, 2017), including *C. socialis* APC12 (red) and L-4 (blue).

Fig. 2 Virus infection dynamics of different *Chaetoceros socialis* strains. (a) Vegetative cell concentration (cells·ml^{-1}) in infected (solid line) and uninfected (dashed line) cultures of strain APC12 isolated from the Mediterranean Sea (red) and strain L-4 isolated off coastal Japan (blue). Strains were infected with CsfrRNAV on day 0. Data shown are mean ± SE of three independent experiments for APC12 and two experiments for L-4, each with three replicates. (b) Viral gene copy number estimated by qRT-PCR at the end of a representative experiment (4 dpi; n=3) in APC12 (red) and L-4 (blue). (c) Infectious units measured by MPN at the end of the same experiment (4 dpi) in APC12 (red) and L-4 (blue). (d) TEM image of ultra-thin section of an infected vegetative cell of strain APC12; chl, chloroplast, n, nucleus, f, frustule; bar, 1 µm. (e) Detail of (d) at higher magnification demonstrating the presence of virus-like particles (arrowed) in the vegetative cell; bar, 0.5 µm. (f) Free viruses in the lysate; bar, 0.1 µm.

Fig. 3 Viral infection induces spore formation in *Chaetoceros socialis*. (a, b) Abundance of vegetative cells (dashed line) and spores (solid line), and percentage of spores (bars) for strain APC12 (red) in infected (a) and uninfected (b) cultures. (c, d) Abundance of vegetative cells (dashed line) and spores (solid line), and percentage of spores (bars) for strain L-4 (blue) in infected (c) and uninfected (d) cultures. Data shown are mean ± SE of three independent experiments for strain APC12 and two experiments for strain L-4, each of them with three replicates. (e) Light micrograph of an AP12 chain of cells with visible resting spores inside the frustules of maternal cells; bar, 10 µm. (f) PCR amplification of the non-structural polyprotein (CSfrRV_gp1) in RNA extracted from triplicate samples of virus-induced spores (infected: 1, 2, 3) from a representative infection experiment; uninfected vegetative cells in exponential growth phase (-); lysates used to infect cells (+). Sizes of

molecular weight markers (mw) are indicated. (g) Ultra-thin sections of a spore of the infected strain APC12; bar, 2 μm.

Fig. 4 Spore formation represses viral propagation in *Chaetoceros socialis*. (a) PCR amplification of CSfrRV_gp1 from: cleaned, virus-induced, spores (v); spores induced by nitrogen starvation (n); fresh virus lysate (l). Sizes of molecular weight markers (mw) are indicated. (b) Extracellular virus abundance before and after washing spores, and 14 days after germination (triplicate samples). (c) Growth curves of germinated cells obtained from infected spores (solid line) and N-limitation (dashed line); data are mean ± SE of three replicates.

Supporting Information

Additional supporting information may be found in the online version of this article.

Fig. S1 Spore formation in nitrogen limitation.

Fig. S2 Time course of the abundance of cells, spores, and virus during infection of strain APC12.

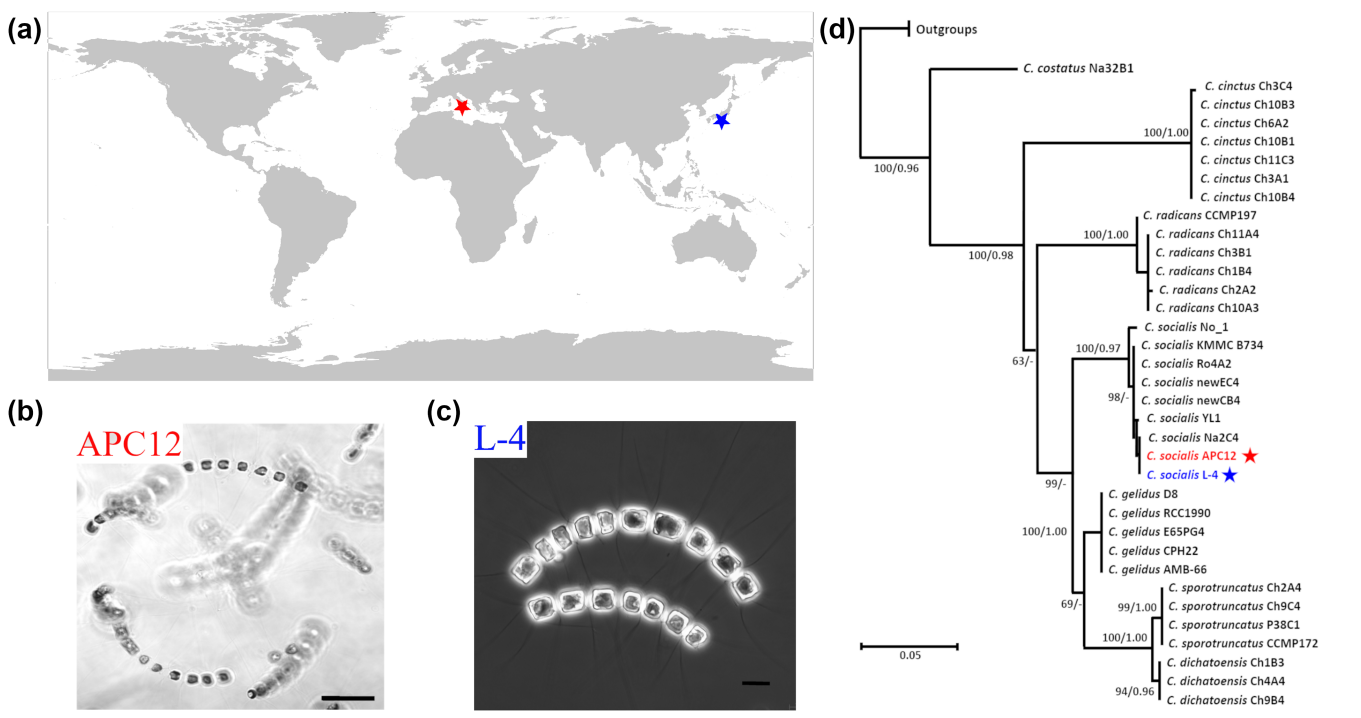
(a)
(b)
APC12
(c)
L-4
(d)
Outgroups
C. costatus Na32B1
C. cinctus Ch3C4
C. cinctus Ch10B3
C. cinctus Ch6A2
C. cinctus Ch10B1
C. cinctus Ch11C3
C. cinctus Ch3A1
C. cinctus Ch10B4
C. radicans CCMP197
C. radicans Ch11A4
C. radicans Ch3B1
C. radicans Ch1B4
C. radicans Ch2A2
C. radicans Ch10A3
C. socialis No_1
C. socialis KMMC B734
C. socialis Ro4A2
C. socialis newEC4
C. socialis newCB4
C. socialis YL1
C. socialis Na2C4
C. socialis APC12
C. socialis L-4
C. gelidus D8
C. gelidus RCC1990
C. gelidus E65PG4
C. gelidus CPH22
C. gelidus AMB-66
C. sporotruncatus Ch2A4
C. sporotruncatus Ch9C4
C. sporotruncatus P38C1
C. sporotruncatus CCMP172
C. dichatoensis Ch1B3
C. dichatoensis Ch4A4
C. dichatoensis Ch9B4
100/1.00
100/0.96
100/1.00
100/0.98
100/0.97
63/-
98/-
99/-
100/1.00
69/-
99/1.00
100/1.00
94/0.96
0.05

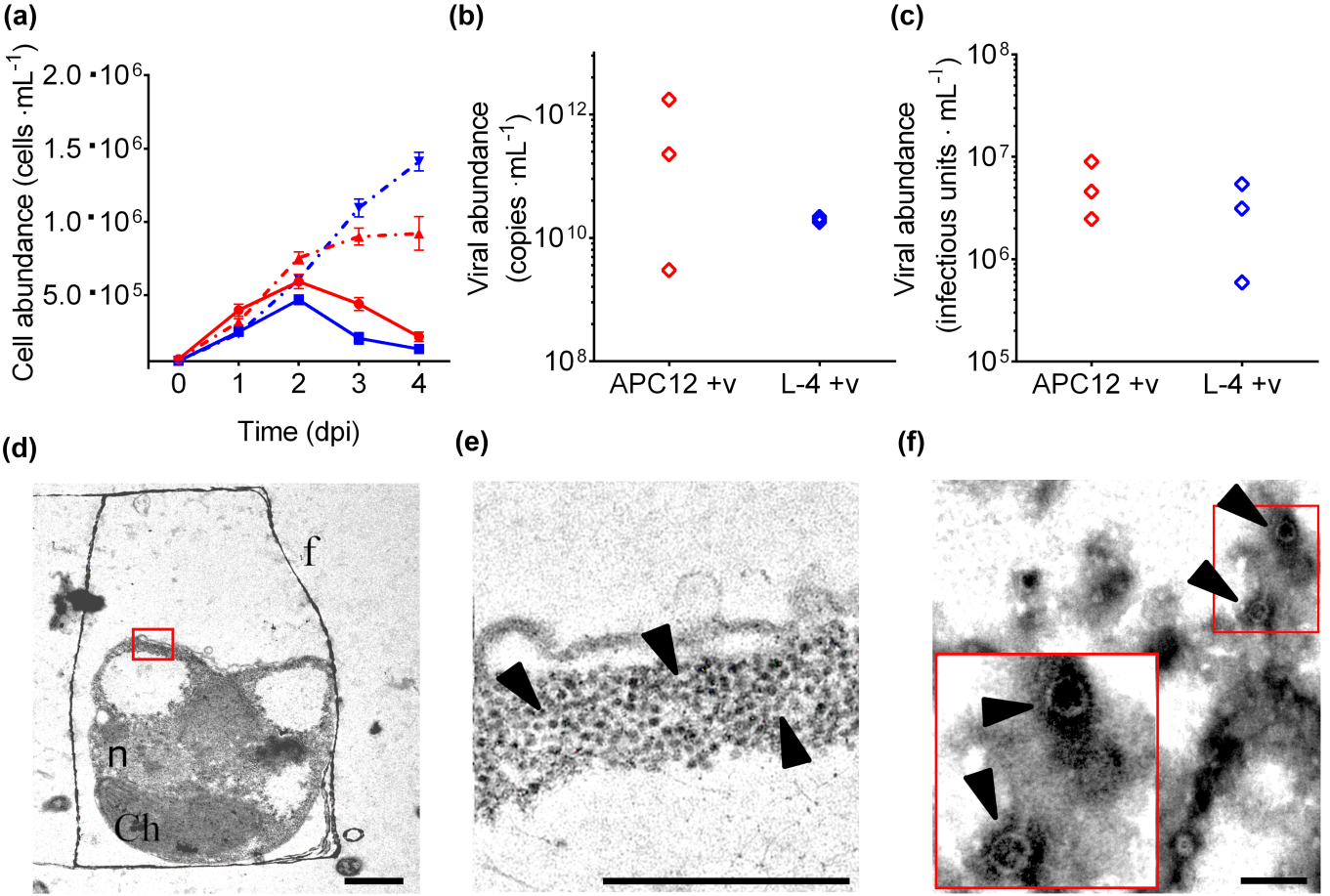
(a)
Cell abundance (cells · mL^{-1})
2.0 · 10^6
1.5 · 10^6
1.0 · 10^6
5.0 · 10^5
0
1
2
3
4
Time (dpi)
(b)
Viral abundance (copies · mL^{-1})
10^{12}
10^{10}
10^8
APC12 +v
L-4 +v
(c)
Viral abundance (infectious units · mL^{-1})
10^8
10^7
10^6
10^5
APC12 +v
L-4 +v
(d)
f
n
Ch
(e)
(f)

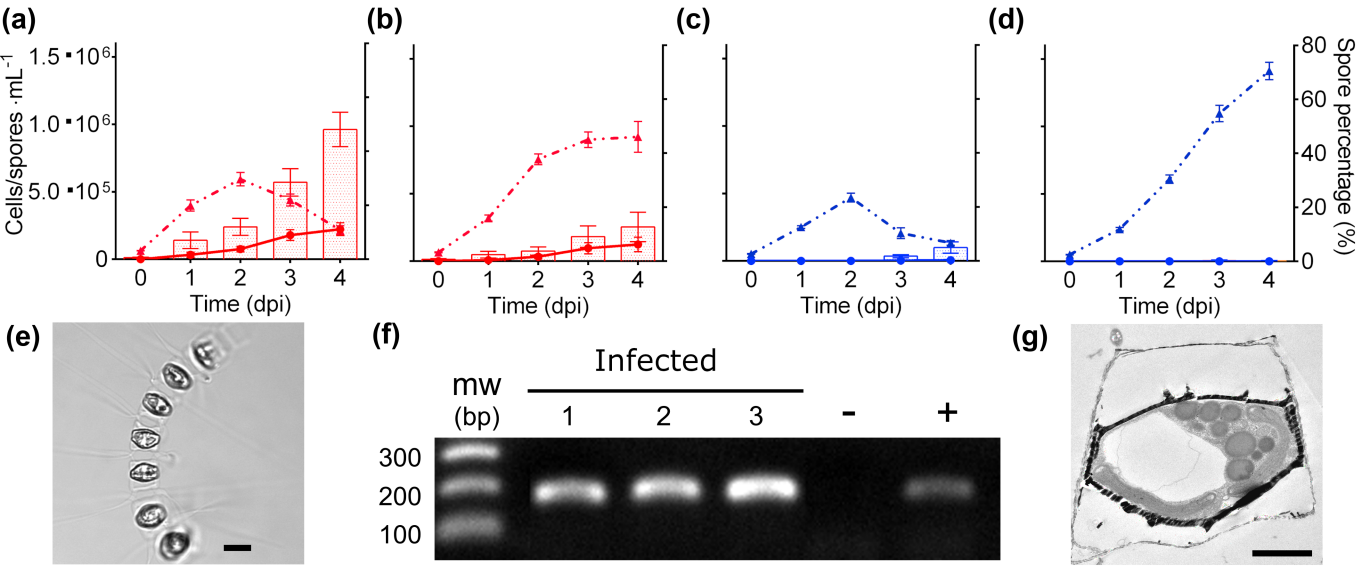
(a)
(b)
(c)
(d)
Cells/spores ·mL-1
1.5 ▪ 10^6
1.0 ▪ 10^6
5.0 ▪ 10^5
0
Spore percentage (%)
80
60
40
20
0
0 1 2 3 4
Time (dpi)
(e)
(f)
Infected
mw
(bp)
1
2
3
-
+
300
200
100
(g)

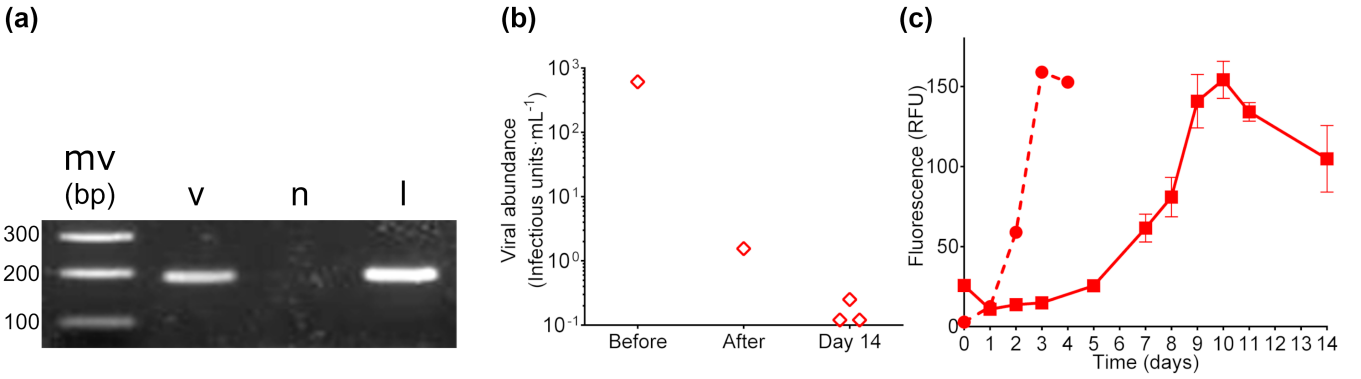
(a)
mv
(bp)
v
n
l
300
200
100
(b)
Viral abundance
(Infectious units·mL-1)
10^3
10^2
10^1
10^0
10^-1
Before
After
Day 14
(c)
Fluorescence (RFU)
150
100
50
0
0 1 2 3 4 5 6 7 8 9 10 11 12 13 14
Time (days)